Physica B 459 (2015) 134–139

Contents lists available at ScienceDirect

Physica B

journal homepage: www.elsevier.com/locate/physb

Theoretical investigation of the electronic structure, optical, elastic and thermodynamics properties of a newly binary boron nitride (T-B_3N_3)

Shibo Zhao [a,*], Jianping Long [b]

[a] Network and Educational Technology Center, Chengdu University of Technology, Chengdu 610059, PR China
[b] College of Materials and Chemistry & Chemical Engineering, Chengdu University of Technology, Chengdu 610059, PR China

ARTICLE INFO

Article history:
Received 6 July 2014
Received in revised form
12 October 2014
Accepted 24 November 2014
Available online 25 November 2014

Keywords:
Metallic boron nitride
Density functional theory
Electronic structure
Elastic constants
Optical properties
Thermodynamic properties

ABSTRACT

The ultrasoft pseudopotential planewave (UPPW) within density functional theory (DFT) has been used to investigate the electronic structure, optical, elastic and thermodynamics properties of newly binary boron nitride (T-B_3N_3). The calculated lattice parameters are in good agreement with previous theoretical results and deviated are less than 0.4%. The electronic structure showed that the T-B_3N_3 is metallic, and the optical spectra exhibit a noticeable anisotropy. The static dielectric constants, optical permittivity constants and the elastic properties are calculated. From our results, we observe that T-B_3N_3 is mechanically unstable and ductile. The entropy, enthalpy, free energy, heat capacity and Debye temperature of T-B_3N_3 was obtained. Up to now, there are no available experimental data about those properties. The results obtained in the present paper could provide important reference data for future studies.

1. Introduction

Binary boron nitride (BN) compounds, attracting a great number of attentions due to their high temperature stability, high melting point, high mechanical strength, large thermal conductivity and useful optical properties, are widely used as a high-temperature ceramic material, insulators and abrasive materials [1–7]. It is interesting to note that BN can form many polymorphs, such as hexagonal BN (h-BN) [8], zinc-blende BN (c-BN) [9,10], wurtzite BN (w-BN) [11], one-dimensional nanostructures [12,13], hollow spheres [14], nanocages [15] and BN nanomesh [16]. At ambient pressure, the c-BN is the most energetically preferred phase. The w-BN is the second stable phase and is always more stable than h-BN. Although w-BN is energetically more stable than h-BN, the energy barrier from h-BN to w-BN is so high that the phase transformation cannot happen at room temperature. The c-BN shows extreme hardness and low dielectric constant while the h-BN is of fundamental importance to study BN nanotubes.

Although B and N element appear to be metallic under high pressure, BN compounds remain an insulator with a wide band gap of around 6.0 eV [17], irrespective of their shape and structure, even when under high pressure [18–20]. The practical application of BN compounds in electronic devices is hindered because of their wide band gap. This has stimulated recent research in reducing or even closing the band gap. Recently, Zhang et al. [21] designed a new tetragonal phase T-B_3N_3, and making the well-known insulating BN become metallic though changes its atomic configuration. To aid in the synthesis of the new phase of T-B_3N_3, Zhang et al. had analyzed of its cohesive energy, electronic structure, density of states and electron localization function. However, the elastic, optical and thermodynamic properties of T-B_3N_3 have not been studied at all. Therefore, the objective of the present work is to investigating these physical properties of T-B_3N_3.

2. Calculation methods

All the calculations presented in the present work have been carried out using the CASTEP code [22], which is an implementation of the ultrasoft pseudopotential plane-wave (UPPW) method, based on the state-of-the-art of density functional theory (DFT). The electronic exchange–correlation interactions are treated with the Perdew–Burke–Ernzerhof for solid in generalized gradient approximation (GGA-PBEsol). [23] The energy with respect to k-points and the cutoff energy have been converged to less than 1 meV. In this study, the cutoff energy of plane-wave is 560 eV, which was large enough to obtain good convergence. B-$2s^2 2p^1$ and N-$2s^2 2p^3$ were explicitly treated as valence electrons. In the Brillouin zone integrations, $14 \times 14 \times 10$ grid of Monkhorst–Pack points has been employed to ensure well convergence of the computed structures and energies. For the calculation of the

* Corresponding author. Fax: +86 2884079530.
E-mail address: zsb@cdut.edu.cn (S. Zhao).

http://dx.doi.org/10.1016/j.physb.2014.11.094
0921-4526/

elastic and optical properties, which usually requires a dense mesh of uniformly distributed k-points, the Brillouin zone integration was performed using a $20\times20\times15$ and $25\times25\times25$ grid of Monkhorst–Pack points, respectively. The equilibrium crystal structures of T-B_3N_3 were determined using the Brodyden–Fletcher–Goldfarb–Shanno (BFGS) [24–27] minimization technique, with the threshold for converged structures: energy change per atom less than 5×10^{-6} eV/atom, the Hellmann–Feynman force per atom less than 0.01 eV/Å and the maximum displacement of atom is 5×10^{-4} Å during the geometry optimization.

3. Results and discussions

3.1. Structure properties

T-B_3N_3 (space group $P\bar{4}m2$ no. 115) has a tetragonal primitive cell containing three formula units [21], as shown in Fig. 1. There are four chemically nonequivalent atoms in the monolayer hexagons BN by sp^2 hybridization. In T-B_3N_3, two interlocked hexagons BN are perpendicular form the special "spiroconjugation" geometry. The optimized lattice parameters and atomic Wyckoff positions of T-B_3N_3 are summarized in Table 1, together with the theoretical results for comparison. The optimized lattice parameters are $a=b=2.63$ Å, $c=6.10$ Å, respectively. They are in good agreement with the theoretical results, and the deviations are 0.38% and 0.16%, respectively. These results show and confirm that the method used in this study is reliable thereby the optimized lattice parameters can be used for future calculations of other parameters.

3.2. Electronic properties

Fig. 2 shows the calculated band structures along the high symmetry directions in the first Brillouin zone (BZ) of T-B_3N_3. The Fermi level (E_f) is chosen to locate at 0 eV and coincides with the top of the valence band (VB). From the Fig. 2, we see that a partially occupied band crosses the E_f in the vicinity of M point, suggesting that the T-B_3N_3 is metallic. To understand the clear picture of the elemental contributions to the electronic structure of T-B_3N_3, we have also computed the total density of states (TDOS) and partial density of states (PDOS) of T-B_3N_3 as given in Fig. 3. As shown in Fig. 3, the obtained value of the TDOS at the E_f is 0.96 electrons/eV. It depicts that the TDOS near the E_f for T-B_3N_3 is dominated by the highly localized N-2p states and a small amount of B-2p states. Our results for band structures and TDOS are similar to other calculations [21]. The VB of the T-B_3N_3 can be divided into two parts. The first part from -21.1 eV to -14.4 eV is mainly due to N-2 s states and minor contributions from B (2s, 2p) states. The second part from -12.4 eV to E_f is mainly due to N-2p states and small contributions of B-2p and B-2s states. The conduction band (CB), from E_f to 26.7 eV, comes primarily from B-2p, 2s states with some contributions from N-2p, 2s states.

Table 1
The lattice parameters and atomic Wyckoff positions of T-B_3N_3.

Atom	Wyckoff positions	Cal.	Ref. [21]
B1	1c	(0.5,0.5,0.5)	(0.5,0.5,0.5)
N1	1b	(0.5,0.5,0.0)	(0.5,0.5,0.0)
B2	2g	(0.0,0.5,0.86037)	(0.0,0.5,0.8602)
N2	2g	(0.0,0.5,0.637842)	(0.0,0.5,0.6378)
a (Å)		2.63	2.64
c (Å)		6.10	6.11

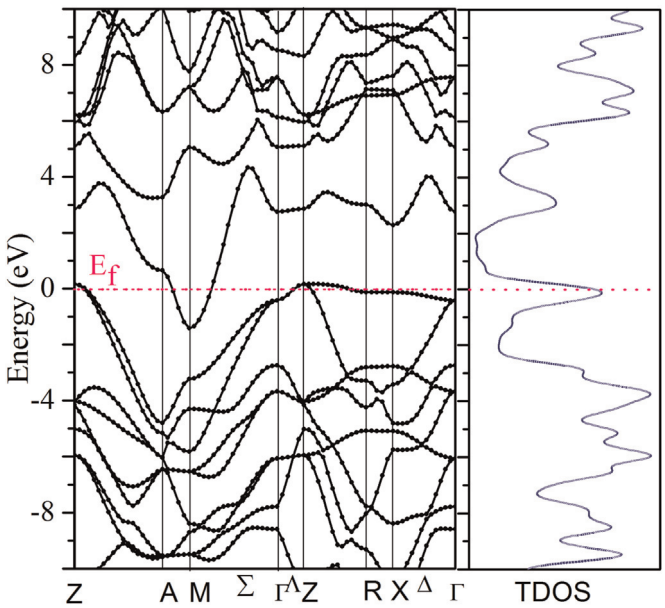

Fig. 2. Band structure and the total density of states of T-B_3N_3.

3.3. Optical properties

The optical properties of T-B_3N_3 are studied by the frequency-dependent dielectric function $\varepsilon(\omega)=\varepsilon'(\omega)+i\varepsilon''(\omega)$ that is mainly connected with the electronic structures. The imaginary part $\varepsilon''(\omega)$ of the dielectric function is calculated from the momentum matrix elements between the occupied and unoccupied electronic. The real part $\varepsilon'(\omega)$ of the dielectric function can be derived from the imaginary part $\varepsilon''(\omega)$ using the Kramer–Kronig relation [28].

The real part $\varepsilon'(\omega)$ and imaginary part $\varepsilon''(\omega)$ of the dielectric function in the energy range from 0 to 20 eV are displayed in Fig. 4. The calculations were performed for two light polarizations along [100] and [001] directions. From Fig. 4, we can see that there are five intensive peaks of absorption centered at about 0 eV, 4.20 eV, 6.02 eV, 9.50 eV and 12.21 eV for the [100] polarization.

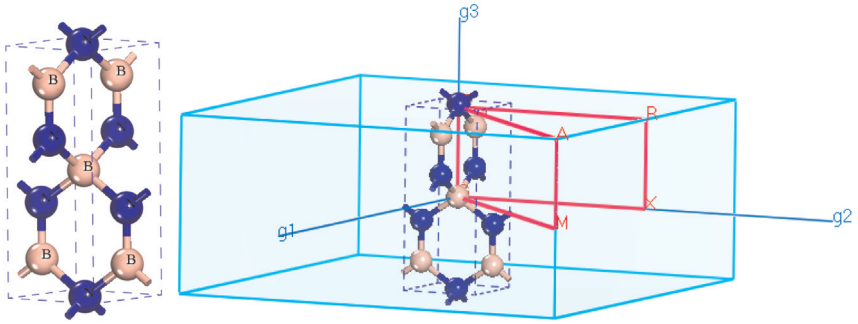

Fig. 1. Crystal structure and the first Brillouin zone of T-B_3N_3.